Arabian Journal for Science and Engineering
https://doi.org/10.1007/s13369-024-09831-8

RESEARCH ARTICLE-CHEMISTRY

Synthesis and Study of the Thermal and Rheological Properties of New Polyepoxide Resin Filled with Carbon Nanotubes

Naoual El-Aouni[1] · Omar Dagdag[2] · Mohamed Berradi[1] · Lahoucine El Gana[3] · Hansang Kim[2] · Avni Berisha[4] · Othman Hamed[5] · Shehdeh Jodeh[5] · Abderrahim El Bachiri[6] · Mohamed Rafik[1]

Received: 28 September 2023 / Accepted: 24 November 2024

Abstract

Continuing our investigation into the synthesis and applications of new epoxy resins, we developed a new octafunctional epoxy resin based on octaglycidyl ether tetra-aniline para methylene dianiline (OGTAPMDA) and investigated its rheological and thermal properties after being reinforced with carbon nanotubes. After manufacturing the resin, we measured its viscometric and rheological properties with an Ubbelohde-type capillary viscometer and a RHM01-RD Haaks rheometer, respectively. To create new nanocomposite materials, the resin was cross-linked thermally with methylene dianiline (MDA) in the presence of carbon nanotubes (CNTs). The thermogravimetric study results allowed us to assess and understand the nature of the heat degradation of these new macromolecular composites. It demonstrates that the thermal stability of the base matrix increases in proportion to the fraction of CNTs. It also shows an increase in the density of the nanocomposites when large amounts of CNTs are utilized, resulting in an increase in polymer viscosity. Rheological investigations of our nanocomposites, on the other hand, show that their thermal and rheological properties are similar. This describes how CNT particles improve the thermal and rheological properties of nanocomposites. The produced nanocomposites' morphology was also examined using the scanning electron microscopy (SEM). The images obtained demonstrate that the carbon nanotubes are evenly distributed in the polyepoxide matrix.

Keywords Epoxy resin · Methylene dianiline · Viscometry · Rheology · CNTs · Nanocomposite · Thermogravimetry

Abbreviations

CNTs	Carbon nanotubes
MDA	Methylene dianiline
OGTAPMDA	Octaglycidyl ether tetra-aniline para methylene dianiline
SEM	Scanning electron microscopy
MD	Molecular dynamics
TGMDA	Tetraglycidyl methylene dianiline
EEW	Equivalent weight of epoxy
AHEW	Equivalent weight of amine hydrogen
PHR	Parts per hundred of resin
TGA	Thermogravimetric analysis
T_d	Temperature of beginning of degradation which corresponds to the loss of 2% in mass
T_{10}	Temperature at the loss of 10% of mass

Naoual El-Aouni and Omar Dagdag are contributed equally to this work.

✉ Hansang Kim
hskim70@gachon.ac.kr

✉ Shehdeh Jodeh
sjodeh@najah.edu

[1] Laboratory of Organic Chemistry, Catalysis and Environment, Department of Chemistry, Faculty of Sciences, University Ibn Tofail, BP 242, 14000 Kenitra, Morocco

[2] Department of Mechanical Engineering, Gachon University, Seongnam 13120, Republic of Korea

[3] Laboratory of Materials Physics and Subatomic, Department of Physics, Faculty of Sciences, Ibn Tofail University, BP 133, 14000 Kenitra, Morocco

[4] Department of Chemistry, Faculty of Natural and Mathematics Science, University of Prishtina, 10000 Prishtina, Kosovo

[5] Department of Chemistry, An-Najah National University, P.O. Box 7, Nablus, Palestine

[6] Royal Naval School, University Department –Boulevard Sour-Jdid, Casablanca, Morocco

Published online: 13 December 2024

T_{50}	Temperature at the loss of 50% of mass
S_{dr}	Rapid degradation threshold
R_{500}	Residual fraction at 500°C

1 Introduction

Epoxy resins are among the most valuable thermosetting polymer materials. They are well renowned for their moisture absorption, high chemical resistance, and good electrical qualities. Their wide range of applications in industries including electronics, aerospace, and automobiles is due to their great mechanical strength and high thermal resistance qualities [1–8]. This has prompted industrial players in these various fields to develop and manufacture new epoxy-family resins while keeping performance, quality, and durability in mind. Indeed, for academic and industrial researchers, synthesizing thermoset polymers with desired qualities is in fact a huge challenge that frequently necessitates a significant investment of time, materials, and scientific resources. The production and development of this kind of thermoset polymer have benefited significantly from advances in this sector that have made it possible to forecast the desired properties of the final nanocomposite material [9].

Predicting and comprehending the diverse properties of epoxy materials necessitates a focus on viscoelastic properties, which have proven to be the most important parameter to consider in prepolymers and their nanocomposites. These properties, in fact, determine the ranges of use of these materials and provide a wide range of reactivity as well as a variety of hardener types [10–12].

These hardeners come in a variety of forms, such as amines and anhydrides. For instance, aromatic amines are crucial in the thermal cross-linking of epoxy resins because they have exceptional chemical resistance, excellent thermal stability, allowing the final material to acquire a very high glass transition temperature [13, 14]. It should be emphasized that a significant relationship exists between the reaction stages epoxy groups with the amine groups and the variation in thermoset viscosity.

Carbon nanotubes (CNTs) have attracted a great deal of interest since their discovery some twenty years ago. This is due to their tubular morphology, nanoscopic diameter, and highly anisotropic character. This particular structure of carbon atoms gives them exceptional properties, particularly in the mechanical, thermal, and electrical fields, making CNTs a prime candidate both for theoretical studies in these areas and for industrial applications exploiting these properties.

Polymer composites can improve the mechanical and thermal properties of neat polymers [15]. Bekhta et al. improved the compressive strength of the cementitious matrix by including ion exchanging resin into the modified novolac epoxy polymer surfactant [16]. In addition, CNTs are a common reinforcing agent in polymer matrices. CNT has outstanding properties, including extremely high strength, stiffness, aspect ratio, and thermal and electrical conductivity [17]. CNTs have been successfully used as a filler in thermosetting polymers (epoxy, phenolic, polyurethane, etc.) and thermoplastic polymers (polyethylene, polypropylene, polystyrene, nylon, etc.) to produce polymer-based composites [18].

In order to exploit these nano-objects on a macroscopic scale, CNTs are used as reinforcements in composite materials, imparting their unique features to the matrix. This work's subject is relevant to this context. The aim is to study the rheological and thermal properties of composite materials based on CNTs in a new epoxy resin matrix. The experimental strategy consisted of first designing and thoroughly characterizing these composite materials. The mechanical properties and thermal conductivity of the composite materials were then simulated using molecular dynamics (MD).

On the other hand, we have previously produced unique epoxy resin-based materials [19, 20]. These materials had good thermal and rheological properties, but we wanted to improve them by designing new materials based on new molecular architectures that included epoxides, aromatic cycles, and nitrogen atoms, and then testing their thermal and rheological characteristics.

2 Materials and Methods

2.1 Synthesis of OGTAPMDA

All chemicals used in this experimental section, such as aniline (99%), epichlorohydrin (99%), methanol (99%), triethylamine (99.5%), methylene dianiline, and carbon nanotube were purchased from Sigma-Aldrich, Germany. All chemicals were used without further purification.

Methylene dianiline para tetra-aniline octaglycidyl ether resin (OGTAPMDA) is developed in two reaction steps. In the first step, tetraglycidyl methylene dianiline (TGMDA) was prepared by condensation reaction between methylene dianiline and epichlorohydrin in the presence of a base. The second step involved adding a nucleophile to the TGMDA, which resulted in the octafunctional resin [21–25]. Figure 1 depicts the reaction scheme for this preparation.

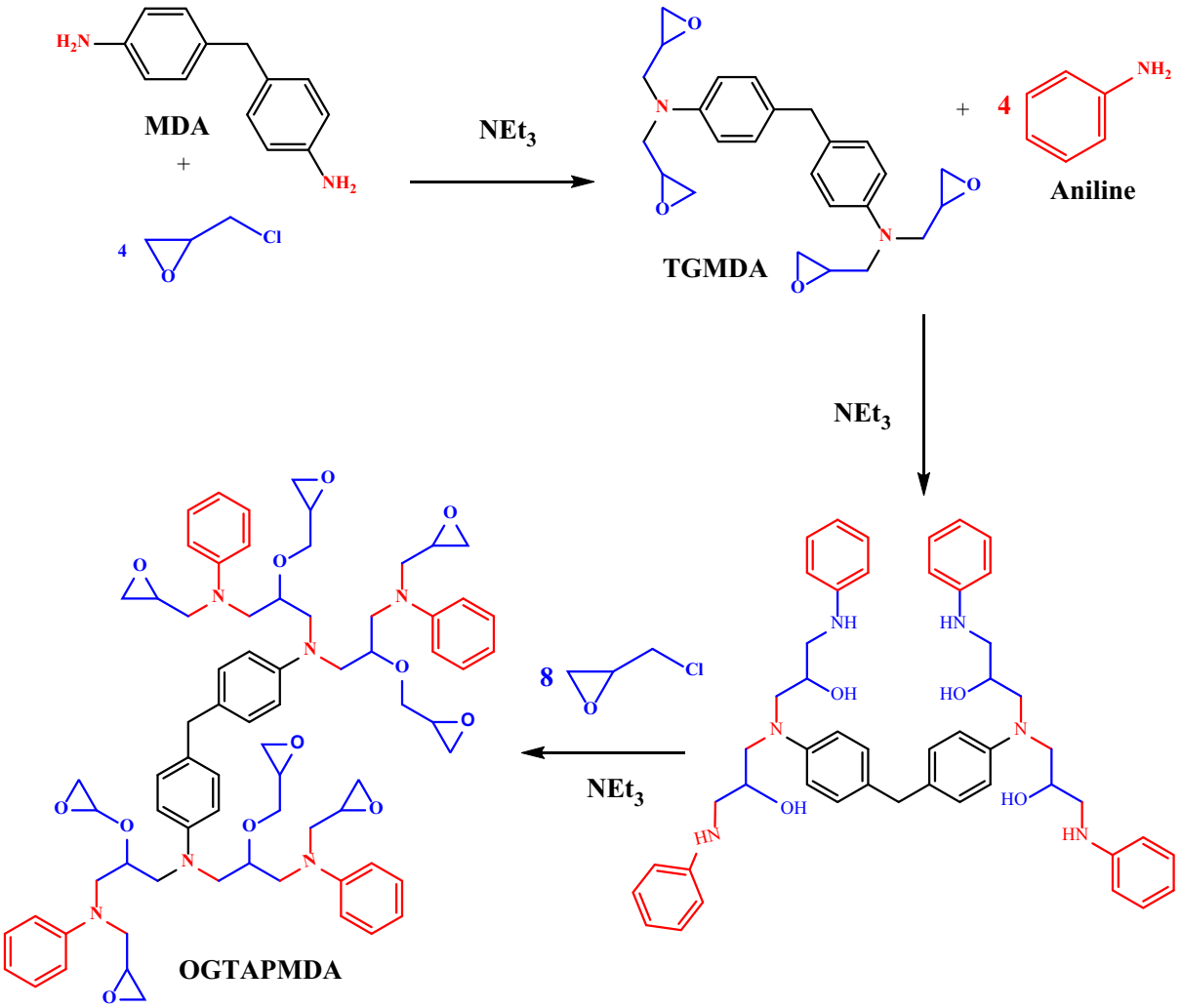

Fig. 1 Synthesis scheme of OGTAPMDA

2.2 Cross-Linking and Formulation of OGTAPMDA Epoxy Resin

Methylene dianiline, which acts as a curing agent throughout the procedure, was used to convert the new epoxy resin into a thermoset material (Fig. 2). Methylene dianiline has an excellent thermal stability and provides exceptional mechanical property to the thermoset polymer [12]. Two amine functions are carried by methylene dianiline, and all four hydrogens are interchangeable. The condensation reactions that take place between the epoxide rings of the polymer and the amine hardener are primarily the cause for the formation of the 3D network [14].

The experimental protocol entails preheating stoichiometric amounts of resin and hardener. The OGTAPMDA resin is heated to 60 °C, while the methylene dianiline is heated to 120 °C. When the methylene dianiline is melted, it is combined with the OGTAPMDA resin to form a single fluid phase. We followed the same procedure to create a hybrid nanocomposite. The latter is created through a reaction of the previously synthesized epoxy resin with methylene dianiline in the presence of carbon nanotubes as reinforcement. Finally, after mixing, we obtained samples with the reinforcement evenly distributed throughout the polymer matrix.

2.3 Stoichiometric Coefficients Ratio of the OGTAPMDA

To acquire the best characteristics, we cured the new octafunctional epoxy resin, octaglycidyl ether tetra-aniline para methylene dianiline (OGTAPMDA), in the presence of methylene dianiline as a curing agent at stoichiometric amounts [26].

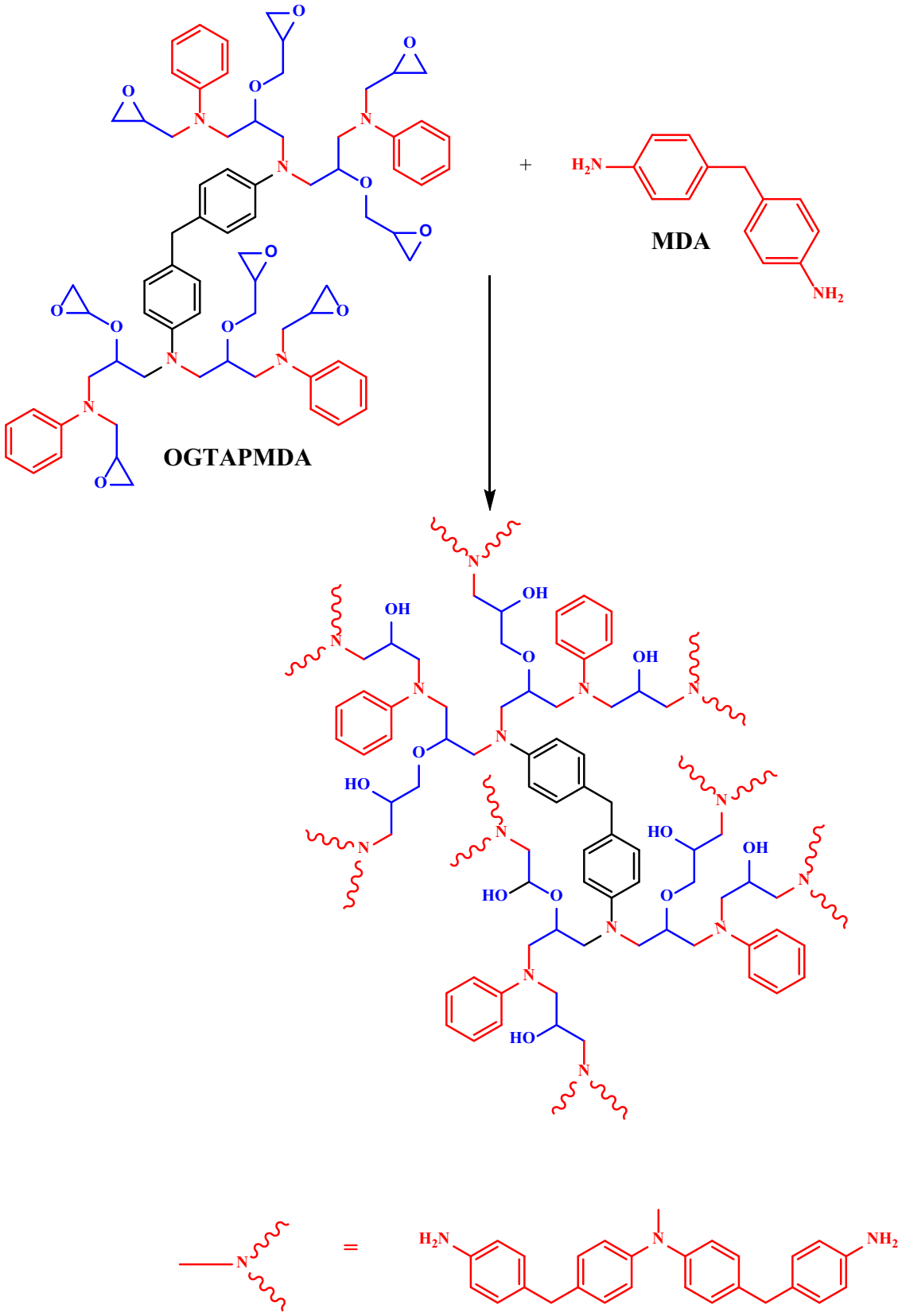

Fig. 2 OGTAPMDA epoxy resin cross-linked by MDA

2.3.1 Equivalent Weight (EEW) of Epoxy

$$EEW = M_w(OGTAPMDA)$$
$$EEW = 1162/8$$
$$EEW = 145.25\, g/eq$$

2.3.2 Equivalent Weight (AHEW) of Amine Hydrogen

$$AHEW = M_w(MDA)/f$$
$$AHEW = 49.5 g/eq$$

2.3.3 Calculation of the Weight Ratio

The weight ratio of the amine hardener to the octafunctional resin, octaglycidyl ether tetra-aniline para methylene dianiline (OGTAPMDA), is calculated as before, per 100 parts of resin (Parts per hundred of resin: PHR) [8, 26]:

$$PHR\ of\ amine = AHEW/EEW$$
$$PHR\ of\ amine = 49.5/145.25 \times 100$$
$$PHR\ of\ amine = 34.07 g/eq$$

According to the calculations of the epoxy equivalent and the amine equivalent, we reacted 34.07 g of MDA for 100 g of octafunctional epoxy resin, octaglycidyl ether tetra-aniline para of methylene dianiline (OGTAPMDA).

2.3.4 Calculation of the Ratio to the Amount of Charge

The desired amount of carbon nanotube filler was calculated according to the following equation [8, 26]:

$$y\% = x/resin + MDA + x$$

x: the amount of octafunctional resin OGTAPMDA, y: the amount of carbon nanotube filler.

2.4 Methods of Analysis

2.4.1 Viscometric Examination

An Ubbelohde viscometer was used to measure the viscosity. The following are the measurement conditions:

- Capillary tube with a 1b viscometer for a series of dilution, k (constant) = 0.051493.
- Temperatures measured in degrees Celsius: 25, 30, 35, 40, 45, 50, and 55
- Each time, three measurements are taken.
- Methanol is the solvent.
- The Hagenbach correction was determined using the formula provided in DIN 51562 1 January 1999 (Measurement of kinematic viscosity by means of the Ubbelohde viscometer).
- The epoxy resin prepolymers were solubilized in methanol with stirring at 25 °C.

2.4.2 Rheological Analysis

The rheological properties of the new octafunctional epoxy resin (OGTAPMDA) were investigated using a HAAKE RHM01-RD rheometer.

2.4.3 Thermogravimetric Analysis

The thermogravimetric analysis (TGA) technique was used to conduct our research on the thermal degradation of epoxy resin nanocomposite materials and the degradation kinetics through mass loss measurements. We used the SETARAM TAG 24 apparatus for this purpose. The temperature rise rate is 10 °C/min^{-1}, with a temperature range from 0 to 600 °C and a balance sensitivity of a 0.5 µg; the measurable mass range was ± 200 mg.

2.4.4 SEM (Scanning Electron Microscopy)

The morphology of our elaborated nanocomposites was observed using a scanning electron microscope. A JEOL-JSM-5500 microscope was employed to make the observations. This method employs a beam of electrons that is accelerated by a fixed potential that excites the surface of the sample. Auger electrons are emitted when the primary electrons are interacted with the material.

2.4.5 Computational Section

In the computational methodology, the study of OGTAPMDA/MDA and OGTAPMDA/MDA/CNTs material was conducted using Materials Studio software. Thermal and mechanical properties were evaluated based on these composite models as depicted in Fig. 3.

Geometry optimization for OGTAPMDA/MDA and OGTAPMDA/MDA/CNTs employed the "Smart" algorithm with "Fine" quality settings. Convergence criteria included energy tolerance of 10^{-4} kcal/mol, force tolerance of 0.005 kcal/mol. Å, stress tolerance of 0.005 GPa, and distance tolerance of 5×10^{-5} Å. The maximum iteration limit was set to

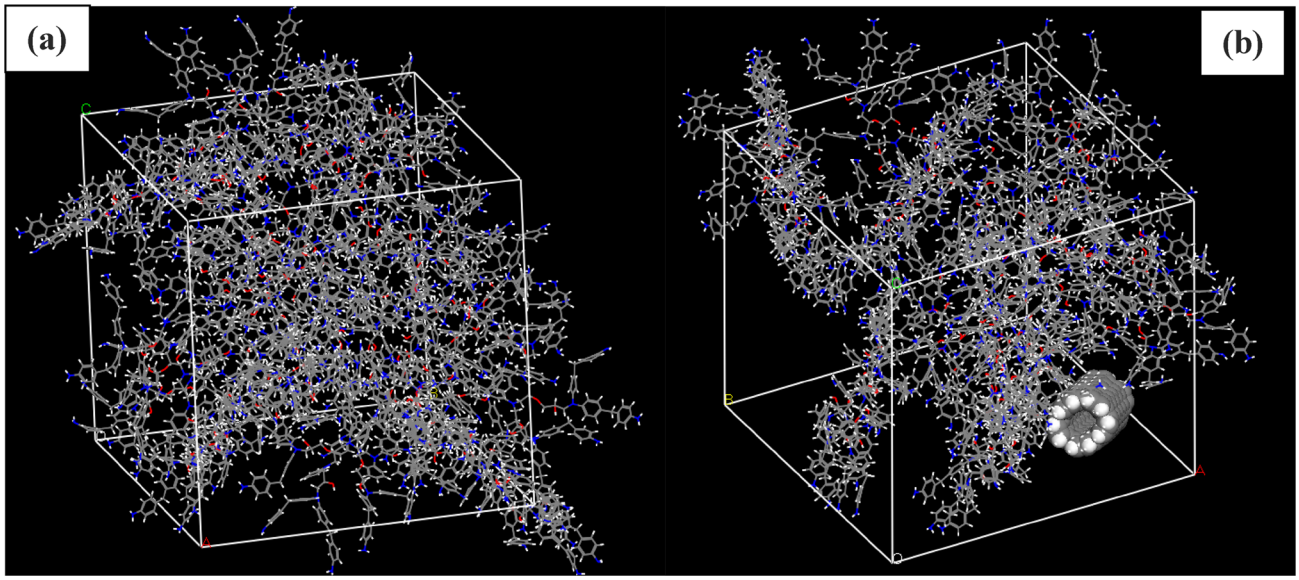

Fig. 3 Models considered for simulations with Amorphous structure **a** of OGTAPMDA/MDA and **b** OGTAPMDA/MDA/CNTs

10^4 for optimization. Energy calculations utilized the COMPASSIII (Version 1.0) forcefield [27], incorporating Ewald summation for electrostatic terms with high accuracy and van der Waals terms computed through atom-based summation. Mechanical property calculations involved a constant strain method with two strains, up to a maximum of 3×10^{-3}. Pre-optimization of the structure preceded mechanical property calculations. In the calculation of mechanical properties, a constant strain method was adopted, with two strain levels considered, and the maximum strain set at 3×10^{-3}. Prior to the mechanical property calculations, structural pre-optimization was performed to ensure accurate results. This approach, conducted within the Materials Studio software, allowed for a comprehensive analysis of the OGTAPMDA/MDA and OGTAPMDA/MDA/CNTs materials.

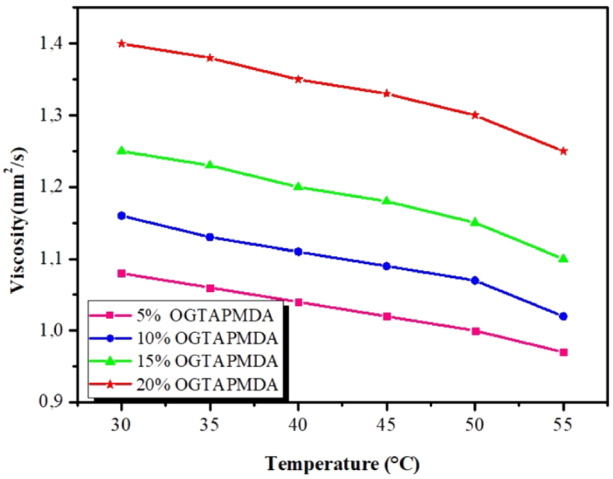

Fig. 4 Variation in viscosity of the epoxy resin, OGTAPMDA as a function of the resin mass percentage at various temperatures

3 Results and Discussion

3.1 Viscosity Study

The viscometric properties of the new octafunctional epoxy resin, octaglycidyl ether tetra-aniline para methylene dianiline (OGTAPMDA), as a function of temperature were primarily investigated. The resin was dissolved in various concentrations of methanol (5%, 10%, 15%, and 20%). We then measured their viscosities with an Ubbelohde VB-1423 capillary viscometer at temperatures ranging from 30 to 55° C. Figure 4 depicts the results obtained from the viscosity of the systems (resin and solvent) as a function of temperature.

According to Fig. 4, the viscosity of the new multifunctional epoxy resin OGTAPMDA increases as polymer mass concentrations increase. This is evident because viscosity rises as the molecular weight of the solute (resin) rises. Furthermore, as the temperature raises, the new OGTAPMDA resin transitions from a viscous sate to a liquid state, explaining the observed drop in measured viscosity. This is due to the higher density of the epoxy resin used in the OGTAPMDA/methanol combination, which results in more interactions between the oxirane rings' C-O bonds and the epoxy resin's Van Der Waals contacts. As the temperature increases, the system's viscosity (OGTAPMDA/methanol) decreases, as expected. It changes from viscous to liquid. As expected, the heat generated by the equipment weakens

the bonds between OGTAPMDA macromolecules, lowering their viscosity. These findings are consistent with those reported by other researchers [12].

Dagdag et al. [12] investigated the temperature-dependent viscometric behavior of four epoxy resins. They demonstrated that the viscometric behavior of phenolic polymers dissolved in chloroform is consistent independent of the temperature of the system. The viscosity of amine polymer systems increases with temperature. This is due to the evolution of the homopolymerization reaction, as the viscometric behavior of the solute increases with molecular weight. Bekhta et al. [28] proved that the viscometric characteristics increase with the weight percentage of the trifunctional epoxy resin, TGETMEP, added to the solution. Other investigations have looked at viscometric properties as a function of mass % and temperature. The viscosity of (epoxy resin/solvent) systems increases in proportion to the polymer [29].

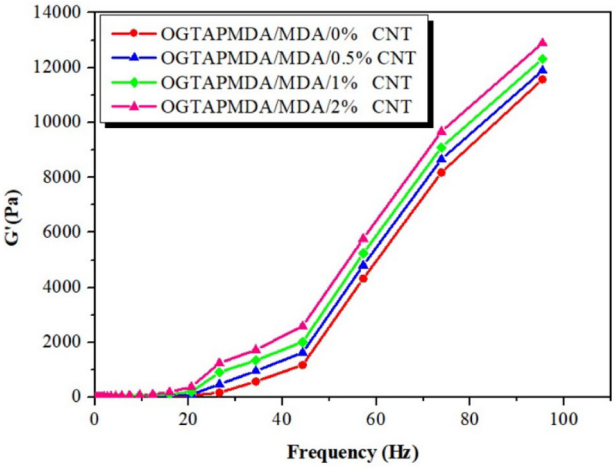

Fig. 5 Elastic behavior as a function of frequency of nanocomposites (OGTAPMDA/MDA/CNTs) at different formulations

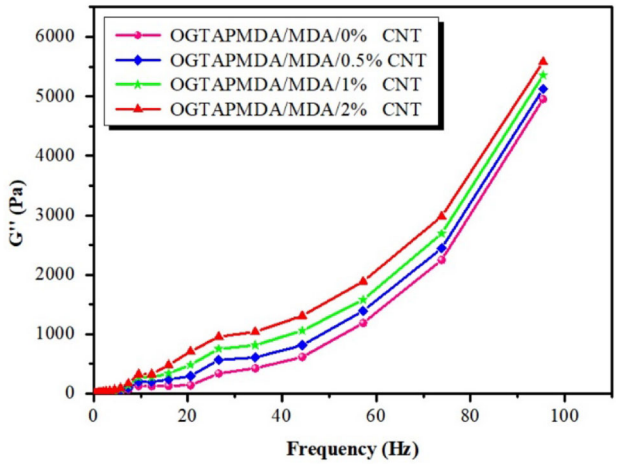

Fig. 6 Variation of glassy behavior *G*" as a function of frequency of nanocomposites (OGTAPMDA/MDA/ CNTs) at different formulations

3.2 Rheological Properties

Determining the rheological properties of the prepared nanocomposites, i.e., the macroscopic viscoelastic behavior, has frequently allowed for a better understanding of the relationship nanocomposites structures and CNTs particle reinforcement of resin. Rheology is thus situated at the crossroads of structural determination and the physical characteristics of nanocomposites. Furthermore, this technique is frequently the key to comprehending and improving the processing.

In this research, we were particularly interested in examining the rheological properties of nanocomposites prepared from CNTs dispersed in an epoxy matrix (OGTAPMDA). We tried to establish at least a qualitative connection between the rheological behavior and the thermal parameters.

In the linear domain at 80 °C and in the frequency range of 0.1 to 100 Hz, the moduli G' and *G*" of the OGTAPMDA/MDA/ CNTs nanocomposites were measured; the findings are shown in Figs. 5 and 6.

Figures 5 and 6 depict the evolution of the two modules of conservation *G*' and loss *G*" as a function of the frequency of solicitation for CNTs mass concentrations ranging from 0 to 2%. Although the addition of carbon nanotubes to the OGTAPMDA prepolymer increases G' significantly, there is only a slight increase in *G*". The physical properties of our formulated materials have been improved as a result of the rheological findings [30].

This is due to an increase in the storage modulus *G*, which indicates that the CNTs in the matrix are well dispersed. An increase in the loss modulus *G*", on the other hand, attests to the persistence of CNTs agglomeration in the system, most likely due to the technique used for dispersion of the nanofiller in the matrix, but the good dispersion of the CNTs, as reflected by the increase in the modulus *G*', remains dominant.

These findings are comparable with those published by Lim et al. [31] for charge dispersion.

Ma et al. [32] identified small CNT aggregation formations in a shear flow that disperse untreated CNTs. In contrast, they found a uniform distribution of treated CNTs. Several researchers investigated the viscoelastic properties of CNT-dispersed systems. Fan et al. [33] define the qualities as the method of dispersion, CNT aspect ratio, concentration, and CNT interaction. As previously mentioned, the dispersed systems given herein exhibit rheological properties that are similar to various other reported results and are considered rheologically normal. The rheological results correspond to better physical properties of the materials we develop. In line with the thermogravimetric results, we find a correlation

between the optimization of rheological and thermal properties as CNT content increases in the matrix. Grich et al. [34] investigated the rheological properties of nanocomposites including dispersed CNT particles in the DGEBA. These rheological properties have shaped the structures and interactions that enable epoxy resins to cure with CNTs [35]. This method is crucial for creating and applying nanocomposites. Various NTC formulations employed in the DGEBA matrix lead to increased G′ and G″ values. The rheological properties of hybrid nanocomposites grew linearly as the percentage of charge added. The authors discovered small aggregated CNT forms in a shear flow of untreated CNT dispersion [36]. On the other hand, they discovered a uniform distribution of treated CNTs. Several writers have demonstrated the properties of distributed CNT systems. The authors discovered that the rheological behaviors were determined by the method of dispersion of CNTs in the polymer matrix [33].

3.3 Thermal Behavior of OGTAPMDA/MDA/CNTs Nanocomposites

Thermogravimetric analysis provides information on a product's thermal stability. The thermograms we acquired allowed us to determine the cured polymer's breakdown temperatures. Furthermore, we provided the properties of this material in accordance with conventional standards [37], as follows:

- T_d: Temperature of beginning of degradation which corresponds to the loss of 2% in mass.
- T_{10}: Temperature at the loss of 10% of mass.
- T_{50}: Temperature at the loss of 50% of mass.
- S_{dr}: Rapid degradation threshold.
- R_{500}: Residual fraction at 500°C.

In order to improve the thermal behavior of the base matrix (OGTAPMDA/MDA), we added carbon nanotubes at various concentrations. The results obtained are represented in Fig. 7.

TGA was used to evaluate the effect of adding CNTs on the thermal stability of epoxy resin. Figure 7 shows the TGA plots of the pure epoxy resin and its nanocomposites reinforced with different wt.% CNTs. From the figures above, the degradation temperature of the pure sample and the nanocomposite samples containing 0.5, 1, and 2 wt.% CNTs is different so that the degradation of the nanocomposite samples occurs at a higher temperature. In other words, by adding CNTs, we can conclude that the thermal stability of the nanocomposite samples is increased. The reason for this can be attributed to the very good thermal stability of CNTs. CNTs are excellent thermal conductors that allow applied heat to transfer through themselves so that the heat is not concentrated in one place, delaying degradation [38].

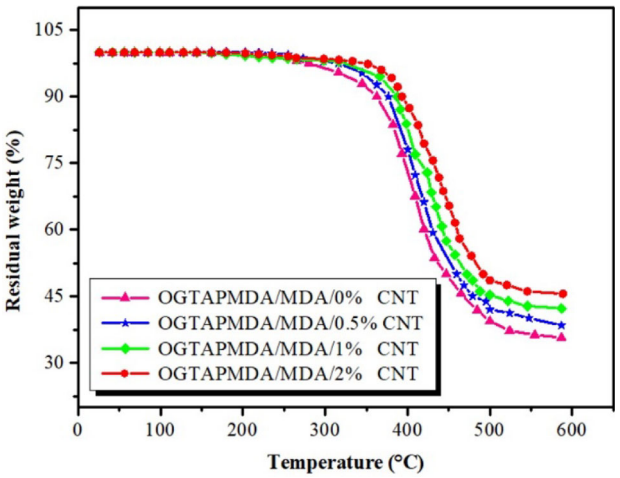

Fig. 7 Thermal properties of OGTAPMDA/MDA/CNTs formulations

These thermograms are comparable, with degradation rates varying according to the rate of CNTs addition. All of these results show that the cured OGTAPMDA resin has good thermal resistance and that the addition of CNT particles has a positive effect on the thermal behavior of the formulated nanocomposites, improving the thermal stability of this epoxy resin. Table 1 categorizes the main thermal properties of these nanocomposites:

As can be seen from Table 1, the weight loss temperature of the nanocomposite samples containing 0.5, 1, and 2 wt.% CNTs equivalent to 10% weight loss of the epoxy sample increased by 19.51, 25.17, and 30.59 °C, respectively, compared to the pure epoxy sample. In addition, the epoxy samples containing 0.5, 1, and 2 wt.% CNTs corresponded to 50% weight loss of the epoxy sample, and the weight loss temperatures increased by 12.59, 25.03, and 44.8 °C, respectively, compared to the pure epoxy sample. The reason for this can be attributed to the very good thermal stability of CNTs and the surface interactions between CNTs and epoxy [39].

A study on pure epoxy resin and CNT-reinforced epoxy matrix nanocomposites showed that by adding 0.5, 1 and 2 wt.% CNTs, the mass loss temperatures of 10% of these materials were 386.07, 396.75, and 409.34 °C, respectively, which is comparable to this work on a similar model [40].

The graph below depicts the evolution of T_d as a function of the percentage of carbon nanotubes (CNTs) (Fig. 8):

The obtained results show that the addition of the filler greatly increases the heat resistance of the formulated thermoset composite. The addition of 0.5% CNTs, for example, raised the onset of OGTAPMDA/MDA/CNTs degradation by 33.02 °C. We also discovered that the percentage of carbon nanotubes added affects thermal stability due to the strong interactions between the CNTs and the epoxy matrix. At the same time, the CNTs act as physical crosslinks and reduce

Table 1 Thermal properties of (OGTAPMDA/MDA/CNTs) formulations

Mass of CNTs (%)	T_d (°C)	T_{10} (°C)	T_{50} (°C)	S_{dr} (°C)	R (%) (500 °C)
0	265,22	362,65	446,96	375,24	39,38
0.5	298,24	382,16	459,55	389	42,03
1	316,51	387,82	471,99	395,34	45,33
2	333,34	393,24	491,76	398,13	48,63

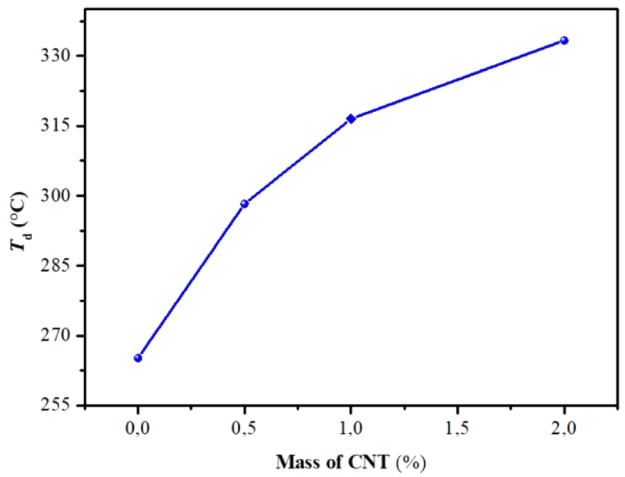

Fig. 8 Evolution of T_d as a function of the percentage of CNTs

the fluidity of the polymer matrix; hence, the glass transition temperature increases [41].

In agreement with the rheological results, we see a correlation between rheological property optimization and thermal property optimization due to the increased CNTs rate in the matrix.

Table 2 displays the thermal properties of epoxy composites as reported by various researchers.

3.4 Morphology of Nanocomposites (OGTAPMDA/MDA/CNT)

The fractured surfaces were examined using SEM to determine the uniformity of the CNT dispersion in the epoxy junction. Figure 9 depicts photographs taken with a scanning electron microscope of the morphology of various formulations of cross-linked thermoset nanocomposites (OGTAPMDA/MDA/CNTs).

SEM images of OGTAPMDA/MDA/CNT nanocomposites at 1 and 2 wt.% demonstrate that carbon nanotube fillers are evenly distributed throughout the matrix. Furthermore, in OGTAPMDA/MDA/CNT nanocomposites, the 2 wt.% filler content has an excellent dispersion [43]. Based on these images and the rheological property measurements, it is possible to predict that at these concentrations, an effective interfacial interaction has developed between the filler and the matrix. This is due to the good distribution and formation of homogenous networks of particles throughout the matrix, resulting in efficient load transfer from the matrix to the fillers. At high concentrations, particles aggregate due to the increased filler-filler propensity and form lumps in the matrix, which function as a defect in the structure of nanocomposites and impair their mechanical and dynamic-mechanical properties [44].

3.5 Theoretical Study

3.5.1 Calculation of Mechanical Properties and Thermal Conductivity

3.5.1.1 Mechanical Properties The simulation of materials using computational methods has become a valuable tool for understanding and predicting their mechanical and thermal properties. In this study, we utilized the Materials Studio software package to investigate the mechanical and thermal conductivity properties of OGTAPMDA/MDA and OGTAPMDA/MDA/CNTs.

The stress–strain relationship of materials can be determined using the generalized Hooke's law [45] as depicted in Eqs. (1):

$$\sigma_i = \boldsymbol{C_{ij}}\varepsilon_j \tag{1}$$

Equation (1) relates to the stress–strain relationship, where σ_i represents the stress, C_{ij} is the calculated elastic stiffness coefficient matrix, and ε_j denotes the strain tensor.

The lame constants λ and μ, as expressed in Eqs. (2) and (3), play a significant role in the formulation [46]:

$$\lambda = \frac{1}{3}(C_{11} + C_{22} + C_{33}) - \frac{2}{3}(C_{44} + C_{55} + C_{66}) \tag{2}$$

$$\mu = \frac{1}{3}(C_{44} + C_{55} + C_{66}) \tag{3}$$

Mechanical properties are crucial indicators of material strength, represented by different moduli. Elastic modulus (E) measures stiffness and deformation resistance, shear modulus (G) indicates shear stress resistance and damage resilience, bulk modulus (K) reflects macroscopic mechanical properties, describing strain–stress connection, and (N)

Table 2 Comparison of the thermal properties of various previous results

Composites	T_d (°C)	T_{10} (°C)	T_{50} (°C)	S_{dr} (°C)	R (%) (500 °C)	Refs
OGTAPMDA/MDA	265	362	446	375	39	This work
OGTAPMDA/MDA/1% CNT	316	387	471	389	45	
TGEHDSEP/MDA	195	374	478	373	38	[20]
TGEHDSEP/MDA/1%NTC	218	396	491	390	44	
TGEDADPBA/MDA	192	281	371	320	25	[19]
TGEDADPBA/MDA/1%ZnO	213	290	390	334	30	
TGEDADPDS/MDA	471	653	744	643	39	[42]
TGEDADPDS/MDA/1%ZnO	486	659	749	647	42	
DGEBA/MDA	212	285	372	342	22	[20]
DGEBA/MDA/1%CNT	232	298	393	360	37	

Poisson's ratio is a measure of the transverse contraction of a material.

The elastic modulus, bulk modulus, shear modulus, and N Poisson's ratio are calculated by molecular dynamics using the below formulas [26, 47]:

$$E = \frac{\mu(3\lambda + 2\mu)}{\lambda + \mu} \tag{4}$$

$$G = \mu \tag{5}$$

$$K = \lambda + \frac{2}{3}\mu \tag{6}$$

$$N = \frac{\lambda}{2(\lambda + \mu)} \tag{7}$$

The mechanical properties of OGTAPMDA/MDA and OGTAPMDA/MDA/CNTs at 300 K, such as Young's modulus, shear moduli, bulk modulus, Poison's ratio, and compressibility, were obtained through MD simulation and are presented in Table 3.

The provided results demonstrate that the Young's modulus of OGTAPMDA/MDA is 0.6921 GPa, while the Young's modulus of OGTAPMDA/MDA/CNTs is significantly higher at 1.3192 GPa. The Young's modulus is a measure of a material's stiffness and its ability to resist deformation when subjected to an applied force. The higher Young's modulus value for OGTAPMDA/MDA/CNTs compared to OGTAPMDA/MDA indicates that the addition of carbon nanotubes (CNTs) to the composite has substantially increased its stiffness and mechanical rigidity.

Certainly, in the context of shear modulus, the results reveal that OGTAPMDA/MDA has a shear modulus of 0.2139 GPa, while the incorporation of carbon nanotubes (CNTs) in OGTAPMDA/MDA/CNTs has notably elevated the shear modulus to 0.3717 GPa. This disparity indicates that the composite with CNTs reinforcement possesses enhanced shear resistance and structural integrity compared to the OGTAPMDA/MDA alone.

Certainly, the comparison of bulk modulus values reveals interesting insights. For OGTAPMDA/MDA, the bulk modulus is noted as − 0.9799 GPa, whereas for OGTAPMDA/MDA/CNTs, it slightly shifts to − 0.8009 GPa. Evidently, the introduction of carbon nanotubes seems to have a mitigating effect on the bulk modulus, making it less negative. This alteration in bulk modulus signifies a nuanced change in the composite's responsiveness to compression, indicating a potential interplay between the matrix and carbon nanotube additives that warrants further exploration.

The calculated Poisson's ratio of 0.6178 for OGTAPMDA/MDA suggests that this material tends to slightly expand laterally when subjected to axial stress, whereas the Poisson's ratio of 0.7746 for OGTAPMDA/MDA/CNTs indicates a relatively higher tendency for lateral expansion under similar conditions, possibly due to the presence of carbon nanotubes enhancing the material's deformation capabilities perpendicular to the applied load.

The compressibility values of 19,552 for OGTAPMDA/MDA and 4615.7742 for OGTAPMDA/MDA/CNTs indicate the materials' ability to be compressed or compacted under pressure. The values provided suggest that OGTAPMDA/MDA/CNTs is more compressible than OGTAPMDA/MDA, potentially due to the addition of carbon nanotubes (CNTs) in the former material.

3.5.2 Thermal Conductivity

Molecular dynamics has been used extensively employed for computing the thermal conductivity of polymeric materials using various approaches [2, 48]. Among these methods, the reverse non-equilibrium molecular dynamics (RNEMD)

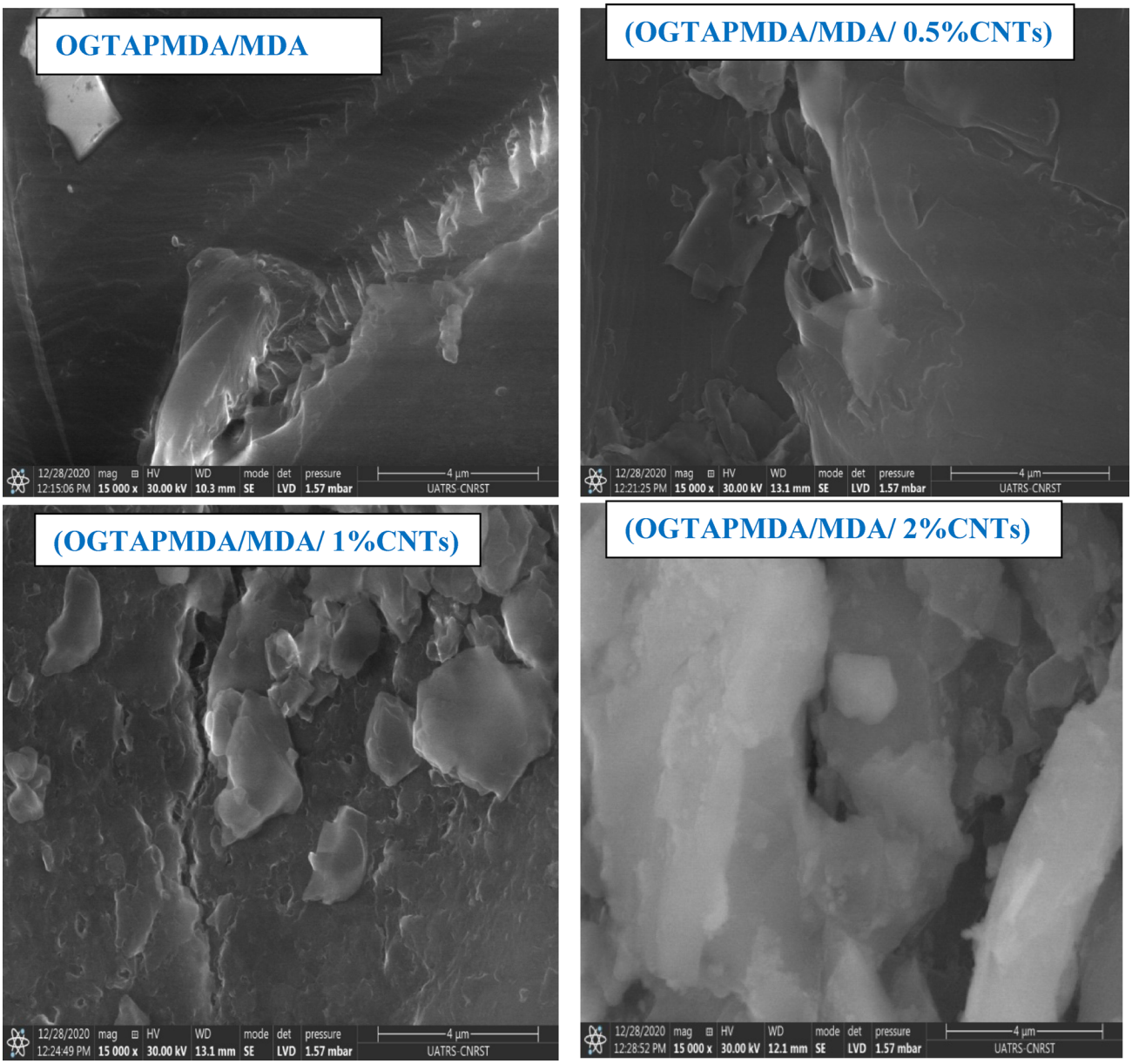

Fig. 9 Photographs of nanocomposites (OGTAPMDA/MDA/CNTs) formulated with different percentages of carbon nanotubes

Table 3 Mechanical properties of OGTAPMDA/MDA and OGTAPMDA/MDA/CNTs

	OGTAPMDA/MDA	OGTAPMDA/MDA/CNTs
Young's modulus (GPa)	0,6921	1,3192
Shear modulus (GPa)	0,2139	0,3717
Bulk modulus (GPa)	− 0,9799	− 0,8009
Poisson's ratio	0,6178	0,7746
Compressibility (1/TPa)	19,552	4615,7742

technique has gained popularity due to its quicker convergence time of temperature gradient [49].

$$\lambda = -\frac{Q}{\mathrm{d}T/\mathrm{d}x} \tag{8}$$

where Q is the energy flux in the x-direction, dT/dx denotes the temperature gradient, and the negative sign signifies that the energy flux is directed opposite to the gradient.

The energy flux is induced by exchanging the energy ΔE between two fixed layers in the system at every time interval Δt. The equation governing this process is as follows:

$$Q = \frac{1}{2A}\frac{\Delta E}{\Delta t} \tag{9}$$

Here, A represents the area perpendicular to the direction of the energy flux, and the factor of 2 arises from the periodic boundary condition.

After equilibrium was attained, the thermal flux caused by the temperature gradient balanced the artificial energy flow, and the temperature profile of the OGTAPMDA/MDA and OGTAPMDA/MDA/CNTs was calculated by time averaging, as shown in Fig. 10.

The thermal conductivity was able to be calculated based on Eqs. (8), (9), as indicated in Fig. 11.

The results were obtained through computational calculations of the thermal conductivity of these materials. The thermal conductivity values of (0.13244 ± 0.0008) W/m/K for OGTAPMDA/MDA and (0.10817 ± 0.0017) W/m/K for OGTAPMDA/MDA/CNTs indicate their respective abilities to conduct heat. This decrease indicates that the presence of carbon nanotubes has influenced the material's heat conduction properties, possibly due to changes in the material's microstructure or phonon scattering effects. The precision of the values is reflected in the narrow uncertainty range, reinforcing the reliability of the measurements.

4 Conclusions

The originality of our study stems from the development of new molecular structures comprising epoxy groups and nitrogen atoms, which are capable of imparting extraordinary qualities to the final materials, particularly thermal stability and adherence to various substrates. On the other hand, the addition of carbon nanotubes to these new resins has substantially improved their qualities. The study of the rheological properties of these materials is also an additional asset of our study.

The current study enabled us to evaluate our epoxy resin and identify the factors that influence the thermal stability of our new thermoset material resin.

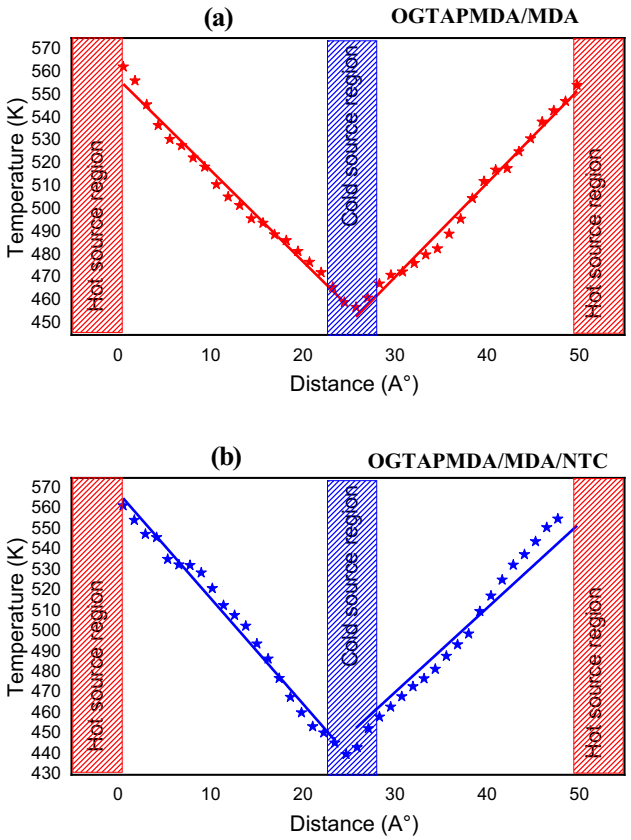

Fig. 10 Variation of temperature distribution **a** of OGTAPMDA/MDA and **b** of OGTAPMDA/MDA/CNTs along z direction (0–50 Å) at 298 K

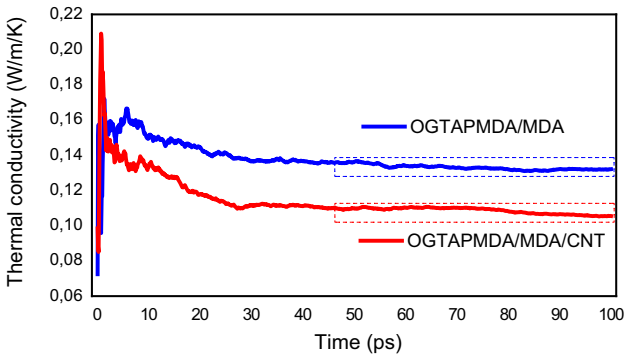

Fig. 11 Simulated thermal conductivity thermal conductivity of OGTAPMDA/MDA and OGTAPMDA/MDA/CNTs

Carbon nanotubes showed the potential to noticeable advantages to epoxy-type polymers, and some drawbacks were identified, such as an increase in the density of the nanocomposites when high levels of CNTs are used, resulting in an increase in the viscosity of the polymer. On the other hand, SEM images of the various prepared nanocomposites (OGTAPMDA/MDA/CNTs) show that the carbon nanotubes are well dispersed in the polyepoxide matrix.

The thermogravimetric measurements of the synthesized nanocomposites reveal a rise in the thermal stability of the base matrix in proportion to the percentage of CNTs, despite the usage of tiny amounts of CNTs.

After the inclusion of carbon nanotubes, rheological examinations of the nanocomposites reveal a similarity between the thermal and rheological properties. This explains how the CNT particles enhance the nanocomposites' thermal and rheological characteristics.

Acknowledgements This research is supported by the "Renewable Energy Core Technology Development Project" of the Ministry of Trade, Industry and Energy (MOTIE) and the Korea Institute of Energy Technology Evaluation and Planning (KETEP) (No. 2022303004020A). In addition, this work was supported by the "Automotive Industry Technology Development Project" of the Ministry of Trade, Industry and Energy (MOTIE) and the Korea Planning & Evaluation Institute of Industrial Technology (KEIT) (No. 20015346).

Authors Contribution Naoual El-Aouni did methodology, software, and investigation. Omar Dagdag done data curation, writing—original draft, and visualization. Mohamed Berradi and Avni Berisha gave software, formal analysis, and data curation. Shehdeh Jodeh and Othman Hamed were involved in writing—review & editing. Mohamed Rafik contributed to conceptualization and resources, writing—review & editing, and project administration. Hansang Kim done conceptualization, methodology, validation, writing—review & editing, and supervision. Abderrahim El Bachiri performed conceptualization, methodology, resources, and writing—review & editing. Lahoucine El Gana and Mohamed Rafik did supervision and project administration.

Declarations

Competing interest The authors declare that they have no known competing financial interests or personal relationships that could have appeared to influence the work reported in this paper.

References

1. Yao, W.; Zhang, Q.; Qi, F.; Zhang, J.; Liu, K.; Li, J.; Chen, W.; Du, Y.; Jin, Y.; Liang, Y.; Liu, N.: Epoxy containing solid polymer electrolyte for lithium ion battery. Electrochim. Acta **318**, 302–313 (2019)
2. El-Aouni, N.; Dagdag, O.; El-Amri, A.; Kim, H.; Haldhar, R.; Kim, S.-C.; Dkhireche, N.; Elbachiri, A.; Berisha, A.; Rafik, M.: Study of new phosphorus-sulfur epoxy polymer for CS anticorrosion in HCl solution: Experimental and theoretical investigations. Mater. Sci. Eng., B **299**, 117011 (2024)
3. Dagdag, O.; Haldhar, R.; Kim, S.-C.; Safi Zaki, S.; Wazzan, N.; Mkadmh, A.M.; Berisha, A.; Berdimurodov, E.; Jodeh, S.; Nwanna, E.E.; Akpan, E.D.; Ebenso, E.E.: Synthesis, physicochemical properties, theoretical and electrochemical studies of tetraglycidyl methylenedianiline. J. Mol. Struct. **1265**, 133508 (2022)
4. Ou, B.; Chen, M.; Guo, Y.; Kang, Y.; Guo, Y.; Zhang, S.; Yan, J.; Liu, Q.; Li, D.: Preparation of novel marine antifouling polyurethane coating materials. Polym. Bull. **75**, 5143–5162 (2018)
5. El-Aouni, N.; Dagdag, O.; El Amri, A.; Berradi, M.; Kim, H.; Elbachiri, A.; Berdimurodov, E.; Berisha, A.; Rafik, M.; Aliev, N.: Experimental and computational insights into destruction protection of E24 carbon metal by new trifunctional sulfur-phosphorus epoxy polymer. J. Taiwan Inst. Chem. Eng. **155**, 105281 (2024)
6. Dagdag, O.; Hamed, O.; Erramli, H.; El Harfi, A.: Anticorrosive performance approach combining an epoxy polyaminoamide-zinc phosphate coatings applied on sulfo-tartaric anodized aluminum alloy 5086. J. Bio Tribo Corros. **4**, 52 (2018)
7. Dagdag, O.; El Harfi, A.; El Gana, L.; Safi, Z.; Guo, L.; Berisha, A.; Verma, C.; Ebenso, E.E.; Wazzan, N.; El Gouri, M.: Designing of phosphorous based highly functional dendrimeric macromolecular resin as an effective coating material for carbon steel in NaCl: Computational and experimental studies. J. Appl. Polym. Sci. **138**, 49673 (2021)
8. Hsissou, R.; Dagdag, O.; Berradi, M.; El Bouchti, M.; Assouag, M.; El Bachiri, A.; Elharfi, A.: Investigation of structure and rheological behavior of a new epoxy polymer pentaglycidyl ether pentabisphenol A of phosphorus and of its composite with natural phosphate. SN Appl. Sci. **1**, 869 (2019)
9. Unnikrishnan, K.P.; Thachil, E.T.: Toughening of epoxy resins. Des. Monomers Polym. **9**, 129–152 (2006)
10. Dagdag, O.; Essamri, A.; El Gana, L.; El Bouchti, M.; Hamed, O.; Cherkaoui, O.; Jodeh, S.; El Harfi, A.: Synthesis, characterization and rheological properties of epoxy monomers derived from bifunctional aromatic amines. Polym. Bull. **76**, 4399–4413 (2019)
11. Dagdag, O.; El Gouri, M.; El Mansouri, A.; Outzourhit, A.; El Harfi, A.; Cherkaoui, O.; El Bachiri, A.; Hamed, O.; Jodeh, S.; Hanbali, G.; Khalaf, B.: Rheological and electrical study of a composite material based on an epoxy polymer containing cyclotriphosphazene. Polymers **12**, 921 (2020)
12. Dagdag, O.; Safi, Z.; Hamed, O.; Jodeh, S.; Wazzan, N.; Haldhar, R.; Safi, S.K.; Berisha, A.; Gouri, M.E.: Comparative study of some epoxy polymers based on bisphenolic and aromatic diamines: synthesis, viscosity, thermal properties computational and statistical approaches. J. Polym. Res. **28**, 165 (2021)
13. Dagdag, O.; El Harfi, A.; Essamri, A.; El Gouri, M.; Chraibi, S.; Assouag, M.; Benzidia, B.; Hamed, O.; Lgaz, H.; Jodeh, S.: Phosphorous-based epoxy resin composition as an effective anticorrosive coating for steel. Int. J. Ind. Chem. **9**, 231–240 (2018)
14. Dagdag, O.; Harfi, A.E.; Essamri, A.; Bachiri, A.E.; Hajjaji, N.; Erramli, H.; Hamed, O.; Jodeh, S.: Anticorrosive performance of new epoxy-amine coatings based on zinc phosphate tetrahydrate as a nontoxic pigment for carbon steel in NaCl medium. Arab. J. Sci. Eng. **43**, 5977–5987 (2018)
15. Manap, A.; Mahalingam, S.; Vaithylingam, R.; Abdullah, H.: Mechanical, thermal and morphological properties of thermoplastic polyurethane composite reinforced by multi-walled carbon nanotube and titanium dioxide hybrid fillers. Polym Bull. **78**, 5815–5832 (2021)
16. Bekhta, A.; Hsissou, R.; Elharfi, A.: Evaluation of Mechanical compressive strength of cementitious matrix with 12% of IER formulated by modified polymer (NEPS) at different percentages. Sci. Rep. **10**, 2461 (2020)
17. Wan, T.; Chen, D.; Bai, X.: Preparation and relative properties of dope-dyed polyurethane modified by β-cyclodextrin. Dyes Pigm. **129**, 18–23 (2016)
18. Zhang, Y.; Zhang, Y.; Liu, Y.; Wang, X.; Yang, B.: A novel surface modification of carbon fiber for high-performance thermoplastic polyurethane composites. Appl. Surf. Sci. **382**, 144–154 (2016)
19. El-Aouni, N.; Dagdag, O.; Haldhar, R.; Kim, S.-C.; Azogagh, M.; Berisha, A.; Sherif, E.-S.M.; Hsissou, R.; Elbachiri, A.; Ebenso, E.E.; Rafik, M.: One-pot synthesis of epoxy resin composite: thermal, rheological and Monte Carlo investigations. Iran Polym J **33**, 435–45 (2024)
20. El-Aouni, N.; Dagdag, O.; Berradi, M.; El Gana, L.; Kim, H.; Berisha, A.; Hamed, O.; Jodeh, S.; El Bachiri, A.; Rafik, M.: Synthesis and study of the thermal and rheological behavior of

carbon nanotubes reinforced new epoxy nanocomposite. Polym. Bull. (2024)
21. El-Aouni, N.; Dagdag, O.; El-Amri, A.; Kim, H.; Berdimurodov, E.; Berisha, A.; Elbachiri, A.; Rafik, M.; Berdimuradov, K.: Synthesis and evaluation of phosphoric ester pyrogallic acid hexaglycidyl ether as a green corrosion protective agent in the gas and oil industries. J. Mater. Sci. **59**, 11057–11078 (2024)
22. El-Aouni, N.; Dagdag, O.; El Amri, A.; Kim, H.; Haldhar, R.; Kim, S.-C.; Dkhireche, N.; El Bachiri, A.; Berisha, A.; Rafik, M.: Synthesis, structural characterization and anticorrosion properties of a new hexafunctional epoxy prepolymer based on urea and phosphorus trichloride for E24 carbon steel in 1.0 M HCl. Colloids Surf. A Physicochem. Eng. Aspects **682**, 132963 (2024)
23. Anon New Hexafunctional Epoxy Prepolymer: Innovation Structure for Corrosion Inhibition. J. Bio- and Tribo-Corrosion
24. El-Aouni, N.; Dagdag, O.; El Amri, A.; Kim, H.; Dkhireche, N.; Elbachiri, A.; Berdimurodov, E.; Berisha, A.; Rafik, M.; Aliev, N.: New hexafunctional epoxy prepolymer: innovation structure for corrosion inhibition. J Bio Tribo Corros **10**, 40 (2024)
25. El-Aouni, N.; Dagdag, O.; El Amri, A.; Kim, H.; Elbachiri, A.; Berdimurodov, E.; Berisha, A.; Rafik, M.; Aliev, N.: Innovative phosphorus-containing epoxy resins: a new approach to acidic corrosion protection. Colloids Surf. A **690**, 133730 (2024)
26. Dagdag, O.; El Gana, L.; Haldhar, R.; Berisha, A.; Kim, S.-C.; Berdimurodov, E.; Hamed, O.; Jodeh, S.; Akpan, E.D.; Ebenso, E.E.: Study on thermal conductivity and mechanical properties of cyclotriphosphazene resin-forced epoxy resin composites. Crystals **13**, 478 (2023)
27. Sun, H.; Jin, Z.; Yang, C.; Akkermans, R.L.C.; Robertson, S.H.; Spenley, N.A.; Miller, S.; Todd, S.M.: COMPASS II: extended coverage for polymer and drug-like molecule databases. J. Mol. Model. **22**, 47 (2016)
28. Bekhta, A.; Hsissou, R.; Bouchiti, M.E.; Harfi, A.E.: Synthesis, structural, viscosimetric, and rheological study, of a new trifunctional phosphorus epoxyde prepolymer, tri-glycidyl ether tri-mercaptoethanol of phosphore (TGETMEP). Mediterr. J. Chem. **6**, 665–73 (2016)
29. Bekhta, A.; Hsissou, R.; Berradi, M.; El Bouchti, M.; Elharfi, A.: Viscosimetric and rheological properties of epoxy resin TGEUBA and their composite (TGEUBA/MDA/TGEMDA+TSP). Res. Eng. **4**, 100058 (2019)
30. El Azzaoui, J.; El-Aouni, N.; Berradi, M.; Hsissou, R.; El Yacoubi, A.; El Bouchti, M.; El Bachiri, A.; El Harfi, A.; Eddine Hegazi, S.; Rafik, M.: Viscometric, rheological, and thermodynamic studies of octafunctional epoxy resins OGDHDPBA and OGDHDPDS. J. Mol. Liq. **384**, 121886 (2023)
31. Lim, H.T.; Ahn, K.H.; Hong, J.S.; Hyun, K.: Nonlinear viscoelasticity of polymer nanocomposites under large amplitude oscillatory shear flow. J. Rheol. **57**, 767–789 (2013)
32. Ma, A.W.K.; Mackley, M.R.; Chinesta, F.: The microstructure and rheology of carbon nanotube suspensions. Int J Mater Form **1**, 75–81 (2008)
33. Fan, Z.; Advani, S.G.: Rheology of multiwall carbon nanotube suspensions. J. Rheol. **51**, 585–604 (2007)
34. Hsissou, R.; Bekhta, A.; Dagdag, O.; El Bachiri, A.; Rafik, M.; Elharfi, A.: Rheological properties of composite polymers and hybrid nanocomposites. Heliyon **6**, e04187 (2020)
35. Hassanzadeh-Aghdam, M.K.; Ansari, R.; Darvizeh, A.: Micromechanical modeling of thermal expansion coefficients for unidirectional glass fiber-reinforced polyimide composites containing silica nanoparticles. Compos. A Appl. Sci. Manuf. **96**, 110–121 (2017)
36. Ma, A.W.K.; Yearsley, K.M.; Chinesta, F.; Mackley, M.R.: A review of the microstructure and rheology of carbon nanotube suspensions. Proc. Inst. Mech. Eng. Part N J. Nanoeng. Nanosyst. **222**, 71–94 (2008)
37. Dagdag, O.; El Gouri, M.; Safi, Z.S.; Wazzan, N.; Safi, S.K.; Jodeh, S.; Hamed, O.; Haldhar, R.; Verma, C.; Ebenso Eno, E.: Flame retardancy of an intumescent epoxy resin containing cyclotriphosphazene: experimental, computational and statistical studies. Iran Polym J **30**, 1169–79 (2021)
38. Najmi, L.; Hu, Z.: Effects of carbon nanotubes on thermal behavior of epoxy resin composites. J. Comps. Sci. **7**, 313 (2023)
39. Du, F.; Guthy, C.; Kashiwagi, T.; Fischer, J.E.; Winey, K.I.: An infiltration method for preparing single-wall nanotube/epoxy composites with improved thermal conductivity. J. Polym. Sci. Part B Polym. Phys. **44**, 1513–1519 (2006)
40. Biercuk, M.J.; Llaguno, M.C.; Radosavljevic, M.; Hyun, J.K.; Johnson, A.T.; Fischer, J.E.: Carbon nanotube composites for thermal management. Appl. Phys. Lett. **80**, 2767–2769 (2002)
41. Ciecierska, E.; Boczkowska, A.; Kurzydlowski, K.J.; Rosca, I.D.; Van Hoa, S.: The effect of carbon nanotubes on epoxy matrix nanocomposites. J Therm Anal Calorim **111**, 1019–1024 (2013)
42. El-Aouni, N.; Hsissou, R.; Azzaoui, J.E.; Bouchti, M.E.; Elharfi, A.: Synthesis rheological and thermal studies of epoxy polymer and its composite. Chem Data Collect. **30**, 100584 (2020)
43. Jojibabu, P.; Jagannatham, M.; Haridoss, P.; Janaki Ram, G.D.; Deshpande, A.P.; Bakshi, S.R.: Effect of different carbon nanofillers on rheological properties and lap shear strength of epoxy adhesive joints. Compos. A Appl. Sci. Manuf. **82**, 53–64 (2016)
44. Du, A.; Zhou, B.; Li, Y.; Li, X.; Ye, J.; Li, L.; Zhang, Z.; Gao, G.; Shen, J.: Aerogel: a potential three-dimensional nanoporous filler for resins. J. Reinf. Plast. Compos. **30**, 912–21 (2011)
45. Tanaka, F.; Okamura, K.: Characterization of cellulose molecules in bio-system studied by modeling methods. Cellulose **12**, 243–252 (2005)
46. Jeyranpour, F.; Alahyarizadeh, Gh.; Arab, B.: Comparative investigation of thermal and mechanical properties of cross-linked epoxy polymers with different curing agents by molecular dynamics simulation. J. Mol. Graph. Model. **62**, 157–164 (2015)
47. Watt, J.P.; Davies, G.F.; O'Connell, R.J.: The elastic properties of composite materials. Rev. Geophys. **14**, 541–563 (1976)
48. Jund, P.; Jullien, R.: Molecular-dynamics calculation of the thermal conductivity of vitreous silica. Phys. Rev. B **59**, 13707–13711 (1999)
49. Liu, X.; Rao, Z.: Molecular dynamics simulations on the heat and mass transfer of hypercrosslinked shell structure of phase change nanocapsules as thermal energy storage materials. Int. J. Heat Mass Transf. **132**, 362–374 (2019)